



This is a repository copy of *Nonlinear Identification and Analysis of Quasiperiodic Oscillations in Reflected Light Measurements of Vasomotion*.

White Rose Research Online URL for this paper:
<http://eprints.whiterose.ac.uk/81818/>

Monograph:

Coca, D., Zheng, Y., Mayhew, J.E.W. et al. (1 more author) (1998) Nonlinear Identification and Analysis of Quasiperiodic Oscillations in Reflected Light Measurements of Vasomotion. Research Report. ACSE Research Report 712 . Department of Automatic Control and Systems Engineering

Reuse

Unless indicated otherwise, fulltext items are protected by copyright with all rights reserved. The copyright exception in section 29 of the Copyright, Designs and Patents Act 1988 allows the making of a single copy solely for the purpose of non-commercial research or private study within the limits of fair dealing. The publisher or other rights-holder may allow further reproduction and re-use of this version - refer to the White Rose Research Online record for this item. Where records identify the publisher as the copyright holder, users can verify any specific terms of use on the publisher's website.

Takedown

If you consider content in White Rose Research Online to be in breach of UK law, please notify us by emailing eprints@whiterose.ac.uk including the URL of the record and the reason for the withdrawal request.



eprints@whiterose.ac.uk
<https://eprints.whiterose.ac.uk/>

X

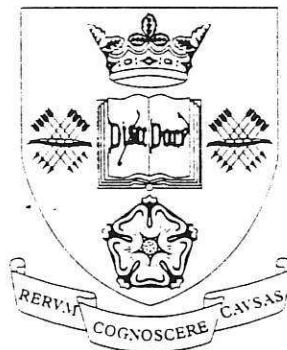
Nonlinear System Identification and Analysis of Quasiperiodic Oscillations in Reflected Light Measurements of Vasomotion

D. Coca, Y. Zheng, J.E.W. Mayhew*, S.A. Billings

Department of Automatic Control & Systems Engineering
University of Sheffield
Mappin Street, Sheffield S1 3JD

*Artificial Intelligence Vision Research Unit
Department of Psychology
University of Sheffield
Western Bank, Sheffield S10 2TP

RESEARCH REPORT



Research Report No. 712
March 1998

200425452



Nonlinear System Identification and Analysis of Quasiperiodic Oscillations in Reflected Light Measurements of Vasomotion

D. Coca, Y. Zheng, J.E.W. Mayhew*, S.A. Billings

Department of Automatic Control & Systems Engineering
University of Sheffield
Mappin Street, Sheffield S1 3JD

*Artificial Intelligence Vision Research Unit
Department of Psychology
University of Sheffield
Western Bank, Sheffield S10 2TP

Abstract

Nonlinear system identification and analysis methods are employed to study the low frequency oscillations present in time series data obtained from reflectance imagery of microvasculature. Using the method of surrogate data testing the analysis reveals the deterministic nature of these oscillations which initially are believed to be chaotic. Further investigations by means of nonlinear system identification techniques indicate however that the underlying dynamics is described very well by a periodically driven nonlinear dynamical model exhibiting quasiperiodic oscillations.

1. Introduction

Numerous studies attest to the fact that low frequency oscillations are present in measurements of blood flow, volume and diameter changes in the microvasculature. The presence of these oscillations has been known and studied for nearly a century (Bayliss 1902 ; Wiedeman 1957). While several low frequency oscillations have been detected, the most frequently reported and studied has a frequency of ~ 0.1 Hz, or 6 cycles/minute, i.e., a period of about 10 seconds. The commonly accepted explanation of the ~ 0.1 Hz oscillations is by mechanisms either myogenic (Folkow 1964; Gustafsson 1993) and/or neurogenic (Golanov, Yamamoto et al. 1994; Golanov and Reis 1995) in origin acting on resistance vessels (arteries and arterioles) to change their diameter with the effect that the modulation of flow rate produces oscillatory changes in saturation and volume. The mechanisms and dynamics underlying these changes in flow rate are complex, and as yet not well understood, and it is uncertain if they have a functional role.

Recently, it has been demonstrated that reflectance changes in video image sequences contained the ~ 0.1 Hz oscillation in areas of brain parenchyma as well as the visible microvasculature (Mayhew, Askew et al. 1996). In a study to be reported elsewhere (Berwick, Askew et al. 1997) image data sequences were collected under 570nm (green) and 660nm (red) wavelength illumination over long durations (up to 40 minutes) from 2mm square regions of cortex and from testes in rat. The genlock of the video camera was used to synchronise the LEDs to capture alternate fields of the video signal at 25Hz which allowed the nearly simultaneous capture of the data under the different illumination conditions. 4000 samples of data recorded under green and red illumination with a sampling frequency of 25Hz are plotted in Figure (1a,b). The raw data was subsequently smoothed to reduce the measurement noise (Figure 1a,b).

Frequency and coherence analysis of the time series of the mean image intensity revealed that the V-signal contained frequency components at $\sim 0.03\text{Hz}$ and $\sim 0.1\text{Hz}$, and there was a reliable phase difference (red leading green by ~ 1.5 secs) in the $\sim 0.1\text{Hz}$ frequency band, but in the frequency band around 0.03Hz the signal under red and green illumination showed no such phase differences. Further analysis revealed a correlation between MABP (Mean Arterial Blood Pressure) and the image time series data in the 0.03Hz frequency band, but no correlation in the $\sim 0.1\text{Hz}$ region of the spectrum.

The finding of the low frequency $\sim 0.03\text{Hz}$ oscillations in our data was to be expected as such low frequencies are known to be present in measurements of cerebral circulation intracranial pressure and arterial blood pressure as well as in vasomotion (Hundley, Renalado et al. 1988; Schmidt, P. Borgstrom et al. 1993; Janssen, Oosting et al. 1995) and also in NAD-NADH redox states (Dora and Kovach 1981).

The results we report here concern the application of nonlinear system identification and analysis techniques to the time series data obtained from reflectance imagery. Several studies have indicated that the vasomotion oscillations have characteristics typical of nonlinear deterministic systems: (Griffith and Edwards 1993; Griffith and Edwards 1994), *in vitro*; Eke LDF in rat cortex; (Tsuda, Tahara et al. 1992) in human pulse; (Cavalcanti and Ursino 1996) arteriolar network models.

The method we describe differs in that we entertain the hypothesis that the $\sim 0.03\text{Hz}$ component of the V-signal signal reflects the variation in blood pressure which modulates flow rate in the local microvasculature and it is the dynamics of these and the underlying capillary beds that gives rise to the $\sim 0.1\text{Hz}$ oscillations present in the V-signal.

To summarise, using nonlinear system identification techniques to analyse the above data we have been able to derive nonlinear models that, when driven by a 0.03Hz periodic input, are able to generate an oscillatory signal qualitatively identical to the V-signal data we measure *in vivo*. The underlying microvasculature can therefore be regarded as a nonlinear oscillator forced with a 0.03Hz periodic input. This model could describe the mechanism behind the rhythmic volume changes in oxygenated and deoxygenated blood in the microvasculature.

We suggest that further exploration along these directions may elucidate further the issues between the myogenic and neurogenic hypotheses of vasomotion.

2. Nonlinear Analysis

It is now well understood that apparent randomness in measured data can be the result of a complex but deterministic underlying mechanism which generate unpredictable or chaotic motion.

In practice it is important to diagnose and characterise such random-like behaviour in order to distinguish between deterministic chaos and stochastic 'noise'. This problem can be reduced to that of performing a number of tests which would indicate that the data are deterministic and possibly chaotic. For example, sensitivity to changes in initial conditions, the fractal properties of the motion in the phase-space, or the existence of unstable periodic orbits, all of which characterise a strange or chaotic attractor, can be investigated by means of computing dynamical invariants such as phase-plots, fractal dimension, Lyapunov exponents or close return maps. In many cases these invariants can be retrieved directly from the experimental observations.

Another important step in characterising the dynamics is extracting from data the mathematical model that describe the observed behaviour. The model which normally reveals the underlying mechanism that generated the data can be used to explain and predict the behaviour of the system under different operating conditions.

2.1 Correlation Dimension Estimation

The correlation dimension (Grassberger 1983) is a quantitative measure which has been successfully used to characterise the fractal dimension of an attracting set.

Essentially, the fractal dimension reflects the fact that the trajectory of a chaotic system in the phase space fills up less than an integer subspace. It follows that a non-integer dimension is the hallmark of a strange attractor.

To compute the correlation dimension the experimental data was used to create the pseudo-phase-space variable $x_i = [x(t_i) x(t_i - \tau) \dots x(t_i - m\tau)]$ where τ is a suitably chosen value of time delay (Rosenstein, J.J. et al. 1993) and m is the embedding dimension. By calculating the distances between pair of points $|x_i - x_j|$ using the Euclidean measure of distance for example, the following correlation function can be defined

$$C(r) = \binom{N}{2}^{-1} \cdot \sum_{0 \leq i < j \leq N} H(r - |x_i - x_j|)$$

where N is the number of data points, $H(s)=1$ for $s>0$ and $H(s)=0$ for $s<0$ and r is the radius of neighbourhood. For a chaotic attractor this function should in principle exhibit a power law dependence $C(r) = ar^{D_c}$ as $r \rightarrow 0$ so the correlation dimension of the attractor D_c can be defined as the slope of the $\log(C)$ versus $\log(r)$ curve

$$D_c = \lim_{r \rightarrow 0} \lim_{N \rightarrow \infty} \frac{\log C(r)}{-\log(r)}$$

Practically D_c is estimated as the slope of the log-log graph of the correlation function $C(r)$ by fitting a straight line to the linear part of the graph known as the scaling region. The scaling region is a critical choice since the dimension estimate can vary significantly by choosing different scaling regions. In practice by computing the correlation function for different embedding dimensions a common scaling region can be identified and used to estimate the dimension.

The correlation dimension was computed using 8000 experimental data samples for five different embedding dimensions. The local slope of the $\log(C)$ vs $\log(r)$ is plotted in Figure (2a) for the experimental signal and in Figure (2b) for a surrogate signal (a random signal with an identical Fourier power-spectrum to the observational signal (Theiler, Eubank et al. 1992)).

While Figure (2a) shows a common plateau for all choices of embedding dimension which corresponds to a correlation dimension $D_c \cong 1.83$ (this is consistent with the fact that the correlation dimension should be independent of the dimension of the embedding space) the local slope for the surrogate data in Figure (2b) does not exhibit such a plateau for any of the embeddings considered.

The results provide a first indication that the experimental signal is a deterministic possibly chaotic signal.

2.2 Lyapunov Exponent Estimation

Chaotic dynamics can be associated with extreme sensitivity of the outcome of the dynamical process to changes in initial conditions. A chaotic system will map at time t a set of initial conditions within a sphere of radius r at time t_0 into an ellipsoid whose major axis grows exponentially $d = re^{\lambda(t-t_0)}$. The largest positive Lyapunov exponent $\lambda > 0$ accounts for the rate of divergence between two nearby trajectories and can be used to establish the chaotic nature of the system under investigation. Normally this exponent can be computed analytically using the equation of motion when known. However, relatively robust strategies for calculating this exponent directly from data are available (Rosenstein, J.J. et al. 1993; Kantz 1994). This involves essentially tracing the exponential divergence of nearby trajectories. Assuming that the observations have been embedded in a space of dimension m , the estimation of λ involves computing the distance function

$$d(k) = \frac{1}{N} \sum_i \frac{\sum_{x_j \in U_r^i} |x_{i+k} - x_{j+k}|}{|U_r^i|}$$

where U_r^i is a r neighbourhood of x_i and $|U_r^i|$ is the number of points in U_r^i . The largest Lyapunov exponent is defined as the slope of the curve $\ln(d)$ versus k . The Lyapunov exponents were computed using 8000 experimental data samples and also the surrogate data set. For the experimental signal the slope of the curve was found to converge towards a common plateau for all choices of embedding dimensions and provided a value of $\lambda \cong 0.103$ for the largest Lyapunov exponent. For the surrogate data set the local slope of the curve $\ln(d)$ versus r was found to be oscillating taking negative as well as positive values.

2.3 Close return maps

Close return maps provide a topological approach to analyse chaotic motion (Mindlin and Gilmore 1992; Gilmore 1993). The basic principle is to search for evidence of unstable periodic orbits which are normally embedded in a chaotic attractor.

Considering $\{x(t_i)\}_{i=1,N}$ to be the time series under investigation, where N is the data length, the possible unstable orbits can be revealed by monitoring the points along the trajectory which are very close (ε -close) in space.

The close return map can be obtained by computing the following matrix

$$C(i, j) = \begin{cases} 1 & \text{if } |x_i - x_{i+j}| < \varepsilon \\ 0 & \text{if } |x_i - x_{i+j}| > \varepsilon \end{cases}$$

where ε is a small positive constant normally $\sim 1\%$ of the signal range. The close return map is obtained by plotting a black dot for every $C(i, j) = 1$.

By checking the close returns different types of motion can be identified (Gilmore 1993). In particular for a chaotic signal a specific pattern containing a number of fragmented horizontal lines will appear in the graphics.

The close return map of the experimental signal shown in Figure (3a) displays a regular pattern where such lines are clearly visible. In contrast, the close return map (Figure (3b)) for the random surrogate data set shows no such regularity of pattern. This illustrates the deterministic, possibly chaotic nature of the experimental signal.

Unlike the first two tests which involve quantitative analysis of the data, the method of close returns is a qualitative test which provide only graphical evidence of deterministic behaviour by exposing periodic orbits embedded within the attractor.

All the tests considered so far clearly indicate the deterministic character of the experimental signal as opposed to the surrogate random data. Although the correlation dimension and the largest positive Lyapunov exponent estimated directly from discrete observations are often not very accurate, the results obtained in this study provide strong evidence of complex dynamical behaviour at the microvasculature level.

3. System Identification

A further step in understanding the nature of the oscillatory vasomotion activity revealed by the experimental measurements is to recover the mathematical equations that model the underlying dynamics. This is a typical nonlinear system identification problem. We have identified both discrete- and continuous-time models from the data. Here only the discrete-time model is discussed.

3.1 Discrete-Time System Identification

In discrete-time, given the set of input/output measurements the task is to recover the difference input/output equation (NARMA model)

$$y(t) = f(y(t-1), \dots, y(t-n_y), u(t-1), \dots, u(t-n_u))$$

which can be augmented to account for the measurement noise in the data (NARMAX model)

$$y(t) = f(y(t-1), \dots, y(t-n_y), u(t-1), \dots, u(t-n_u), e(t-1), \dots, e(t-n_e))$$

(Leontaritis and Billings 1985; Leontaritis and Billings 1985) where y , u , e are the input, output and noise respectively, n_y, n_u, n_e are the maximum input, output and noise lags and $f(\cdot)$ is an unknown nonlinear function. In practice it is convenient to represent $f(\cdot)$ as a polynomial function in y , u , and e . Polynomial models have a simple structure, provide a closed-form for the model and can be used to represent a wide class of nonlinear systems (Chen and Billings 1989). Moreover, the polynomial representation is linear-in-the-parameters so that the unknown parameters can be estimated easily using least-squares algorithms.

However, a model that contains all possible polynomial terms is normally too complex for a given identification problem. A major task therefore is to select the correct terms with which to implement the model. An effective solution is to use an orthogonal

forward regression algorithm to perform model structure selection and parameter estimation. For a complete description of the algorithm see Billings(1989).

3.2 The Discrete-Time Model

A number of physiological studies have suggested the existence of a pacemaker (periodic forcing input) as a possible cause of the random-like fluctuations observed in the blood flow in the microvasculature.

In our study we have found that autonomous models (with no external forcing) estimated from data could not adequately capture the observed behaviour. The structure selection and parameter estimation algorithms, have produced in this case only models which exhibit a limit cycle behaviour similar to that displayed in Figure (4). The power spectral density of the periodic output in this case is mainly concentrated at ~ 0.1 Hz frequency. In contrast, although the power spectral density of experimental data has also revealed the presence of a low frequency component ~ 0.03 Hz with the same phase in the experimental time series under green and red illumination, this frequency component was absent from the output of all estimated autonomous models.

Motivated by these observations and by the fact that the experimental data was found to be strongly correlated with the arterial blood pressure at this particular frequency a periodic signal with ~ 0.03 Hz frequency, assumed to act as an external forcing input for the system, was used to estimate discrete-time models from the data. The amplitude and phase information of the input signal were obtained by least-square fitting a sine and cosine function with the frequency ~ 0.03 Hz to the experimental 'red' data after the mean was removed. The data sets used for estimation consisted of 2×1000 data points recorded under green and red illumination with a sampling period $dt=0.16$ s.

A number of discrete-time models driven by the periodic perturbation extracted from data were estimated using experimental measurements from different experiments. In each case the discrete-time models, represented as a system of two nonlinear difference equations, could reproduce very well the observed behaviour. An example of such model estimated from the data plotted in Figure (1a,b) is given below

$$\begin{aligned}
 g(t) = & -1.768485668 \cdot 10^3 g(t-1) + 5.622859414 \cdot 10^{-2} r(t-1)^3 \\
 & -1.553273185 \cdot 10^{-1} g(t-1)r(t-1)^2 + 1.467159577 \cdot 10^5 \\
 & + 5.948968435 \cdot 10^{-2} g(t-1)^2 u(t-1) + 6.068632954 \cdot 10^{-3} g(t-1)^2 r(t-1) \\
 & -1.228501546 \cdot 10^2 r(t-1)u(t-1) - 7.093971541 \cdot 10^{-1} g(t-1)^2 \\
 & + 33.26112571 g(t-1)r(t-1) - 2.019333975 \cdot 10^3 r(t-1) - 14.78316977 g(t-1)u(t-1) \\
 & + 7.705688293 \cdot 10^3 u(t-1) + 5.558352824 \cdot 10^{-1} r(t-1)^2 u(t-1) \\
 r(t) = & 7.997723476 r(t-1) - 1.13256518 \cdot 10^2 g(t-1) - 2.736708735 \cdot 10^{-3} g(t-1)^3 \\
 & + 4.273082457 \cdot 10^3 + 1.041728814 \cdot 10^{-3} g(t-1)^2 r(t-1) \\
 & - 8.297871391 \cdot 10^{-4} g(t-1)r(t-1)^2 + 8.911030068 \cdot 10^{-1} g(t-1)^2 \\
 & + 4.620629966 \cdot 10^{-2} g(t-1)u(t-1)^2 + 1.155881205 \cdot 10^{-2} g(t-1)^2 u(t-1) \\
 & + 1.45511184 \cdot 10^{-2} r(t-1)^2 u(t-1) - 2.567488992 \cdot 10^{-2} g(t-1)r(t-1)u(t-1) \\
 & - 2.993158072 \cdot 10^{-2} g(t-1)u(t-1) - 5.281090196 u(t-1)^2
 \end{aligned}$$

where g and r are the signals under green and red illumination and u is a ~ 0.036 Hz periodic input with amplitude $A \sim 0.15$.

4. Model Validation

The ability of the estimated model to reproduce the observed dynamical behaviour can be judged by comparing the phase-space portraits plotted in Figures (5a,b) using the experimental signals and the model simulated outputs. The one-step-ahead predicted outputs and the model simulated outputs are also compared with the estimation data in Figures (6a,b) and (7a,b) respectively.

The correlation dimension and the largest Lyapunov exponent of this model were computed using 8000 data samples generated by the model. The values found $D_c \cong 2.03$ and $\lambda \cong 0.098$ are similar to those estimated directly from the data. Moreover, the close return map computed for the 'green' model simulated output (Figure 9) is very similar to the return map obtained for the experimental 'green' signal (Figure 3a).

At this stage, following long term simulation, it was apparent that the behaviour of the model is aperiodic but stable. This is normally associated with either chaos or quasiperiodicity.

A simple way to expose the underlying structure of the aperiodic attracting set and distinguish between chaotic and quasiperiodic motion is to compute a Poincaré map for the system. In this case, the Poincaré map computed for the estimated model (Figure 10) reveals a smooth, closed curve which proves the quasiperiodic nature of the attractor. Observe in this case the similarity between this Poincaré map and the limit cycle plotted in Figure (4). This illustrates the fact that the observed irregular oscillations are caused by the interaction between an intrinsic periodic behaviour (probably characteristic to the microvasculature) and an external perturbation at ~ 0.03 Hz (probably caused by blood pressure fluctuations).

5. Discussion and Conclusions

The major findings of the present study relate to the nature and cause of the irregular oscillations exhibited by the V-signal. Using nonlinear mathematical techniques we were able to quantify the complexity of irregular time series (V-signal) through computation of quantitative and qualitative dynamical invariants such as correlation (fractal) dimension, the maximal Lyapunov exponent and by plotting the close return maps. The results obtained for the experimental measurements, which clearly contrast with the results obtained for surrogate random data, strongly indicate the deterministic character of the oscillations. These initial findings confirmed previous investigations in this area that suggested that the oscillations are deterministic, possibly chaotic.

Establishing the chaotic nature of a signal based only on numerical computation of dynamical invariants it is often not very convincing. For this reason, system identification techniques were employed in an attempt to extract from the data a mathematical model that could provide further insight into the nature of the oscillations.

In a first stage nonlinear discrete-time models with no exogenous inputs were fitted to the data. These models however could not reproduce adequately the observed behaviour. In particular, all these models exhibited a limit cycle behaviour which suggested the need of an external input.

This hypothesis proved to be fruitful since the discrete-time models derived from the V-signal using as an input a $\sim 0.03\text{Hz}$ periodic input could reproduce remarkably well the qualitative and quantitative features of the experimental signals.

The choice of the external input was motivated by the fact that the 0.03Hz oscillation in the data correlate strongly with the mean arterial blood pressure (MABP) and has the same phase for both signals obtained under green and red illumination. Moreover the 0.03 Hz oscillation could not be detected in the simulated output of the autonomous models estimated from data which indicate that it is an exogenous signal.

In general a nonlinear oscillator when forced with an external periodic input can exhibit aperiodic oscillations which in principle could be chaotic or quasiperiodic. For a long time it was believed that the observed irregular behaviour is chaotic. The analysis presented in this paper however, provides strong evidence that the oscillations are in fact quasiperiodic. This points out the shortcomings of relying only on dynamical invariants computed directly from data to detect or classify chaotic dynamics. The computation of these invariants however was clearly useful in establishing the deterministic nature of the experimental data. The correlation dimension in particular clearly indicated the nontrivial character of the dynamics in the state-space. It is worth noting that both quasiperiodic and chaotic attractors have dimensions greater than that of a simple limit cycle.

Based on the results presented in this study it is possible to speculate that the vasomotion oscillations in the absence of the 0.03 Hz input are described by an autonomous dynamical system with a periodic limit cycle. This natural limit cycle seem to interact with an exogenous 0.03Hz excitation, which probably is related to the fluctuations of the blood pressure, resulting in the observed quasiperiodic oscillations. The physical interpretation of the nonlinear model however is not that trivial. By using naive oximetry for example the green and red signals could be transformed easily into blood volume and saturation (the ratio of oxygenated and deoxygenated haemoglobin) oscillations. In such case a similar nonlinear model was found to describe the volume and saturation oscillations. Again, the quasiperiodic nature of the model suggests that in the absence of the periodic perturbation at 0.03Hz the volume and saturation oscillations would have a limit cycle behaviour which seems to be intrinsic to the microvasculature. An interesting question is whether the 0.03Hz oscillation has a functional role at the microvasculature level or is just an accidental perturbation.

Multi-wavelength spectrographic analysis however, (Berwick, Askew et al. 1997) shows that at wavelengths below 590nm , by far the major component of the changes in absorption contributing to the V-signal is wavelength independent and due to changes in scattering (See Figure (11)). In the case of the data under the red illumination ($\sim 660\text{nm}$) we believe that it confounds both the wavelength independent scattering and changes in absorption derived from changes in the oxygenation of haemoglobin (and possibly from changes in the state of oxidation of the cytochromes involved in the metabolic electron transport chain). If so, subtracting the green from the red V-signal would produce a signal derived predominantly from saturation and metabolic changes whilst the green signal oscillations will represent mainly changes in scattering.

Figure (11a) shows the spectral variation in the V-signal over time from a different study. Figure (11b) shows time series of the absorption at 570nm and 650nm and, for comparison, the absorption changes due to the oscillation in the tissue scattering obtained using Nonlinear Multi-Component Analysis (NLMCA) (Heinrich, Hoffman et al. 1987; Mayhew, Zhao et al. 1997). Figure (11c) shows the changes in cytochrome

oxidation and in oxygenated haemoglobin from the same analysis superimposed on the difference between the red and green V-signal measurements.

Under either of these interpretations, physically meaningful variables could be derived from the green and red signals by an appropriate transformation. This however would not change the intrinsic nature of the dynamics.

A fuller interpretation of the implications of this analysis is impossible at this state of knowledge not least given the uncertainty concerning the origins of the intrinsic signal sources and the physiological meaning of the optical V-signal time series data used in the modelling process. However the results concerning the nature of the system and its nonlinear characteristics should hold under different transformations of the measurement data. Thus the conclusions concerning the quasiperiodic nature of the oscillations are maintained whether we use naïve oximetry to transform the time series data into estimates of volume and saturation or scattering and saturation.

Acknowledgements

The authors gratefully acknowledge the members of the Brain Imaging Group at Sheffield University for access to their data and for help in the preparation of this paper. The research was funded by EPSRC grant No. GR/L 35386.

References

- Bayliss, W. M. (1902). "On the local reactions of the arterial wall to changes in internal pressure." *J. Physiol.* **28**: 220-.
- Berwick, J., S. Askew, et al. (1997). "Optical imaging of V-signal oscillations in the microcirculation of the rat cerebral cortex and testes." *Neurosciences Abstracts* J-67.
- Billings, S. A., S. Chen, et al. (1989). "Identification of MIMO nonlinear systems using a forward-regression orthogonal estimator." *Int J. of Control* **49**: 2157-2189.
- Cavalcanti, S. and M. Ursino (1996). "Chaotic oscillations in microvessel arterial networks." *Annals of Biomedical Engineering* **24**: 37-47.
- Chen, S. and S. A. Billings (1989). "Representations of nonlinear systems: the Narmax model." *Int J. of Control* **49**: 1605-1629.
- Dora, E. and A. G. B. Kovach (1981). "Metabolic and vascular volume oscillations in the cat brain cortex." *Acta Physiol. Acad. Sci. Hun.* **57**(3): 261-275.
- Folkow, B. (1964). "Description of the myogenic hypothesis." *Circ. Res.* **20**: 327-335.
- Gilmore, R. (1993). "A new approach for testing for chaos, with applications in finance and economics." *Int. J of Bifurcation and Chaos* **3**: 583-587.
- Golanov, E. V. and D. Reis (1995). "Vasodilation evoked from medulla and cerebellum is coupled to bursts of cortical EEG activity in rats." *J. Am. Physiol.* **268** (**Regulatory Integrative Comp. Physiol.** **38**): R454-R467.
- Golanov, E. V., S. Yamamoto, et al. (1994). "Spontaneous waves of cerebral blood flow associated with a pattern of electrocortical activity." *J. Am. Physiol.* **266** (**Regulatory Integrative Comp. Physiol.** **35**): R204-R214.
- Grassberger, P. a. P., I (1983). "Measuring the strangeness of strange attractors." *Physica D*: 189-208.
- Griffith, T. M. and D. H. Edwards (1993). "Mechanisms underlying chaotic vasomotion in isolated resistance arteries: roles of calcium and EDRF." *Biorheology* **30**: 333-347.

- Griffith, T. M. and D. H. Edwards (1994). "Fractal analysis of roth of smooth muscle Ca fluxes in genesisi of chaotic arterial pressure oscillations." Am. J.Physiol. **266 (Heart Circ. Physiol.)**: H1801-H1811.
- Gustafsson, H. (1993). "Vasomotion and underlying mechanisms in small arteries." Acta Physiologica Scandinavica **149 (Suppl. 614)**: 1-44.
- Heinrich, U., J. Hoffman, et al. (1987). "Quantitative evaluation of optical reflection spectra of blood-free perfused guinea pig brain using a nonlinear multicomponent analysis." Pflugers Arch. **409**: 152-157.
- Hundley, W. G., G. J. Renalado, et al. (1988). "Vaosmotion in cerebral microcirculation of awake rabbits." Am. J. Physiol. **254(23)**: H67-H71.
- Janssen, B. J. A., J. Oosting, et al. (1995). "Hemodynamic basis of oscillations in systemic arterial pressure in conscious rats." Americal Journal of Physiology **269**: H62-H71.
- Kantz, H. (1994). "A robust method to estimate the maximal Lyapunov exponent of a time series." Phys. Rev. A. **185**: 77-87.
- Leontaritis, I. J. and S. A. Billings (1985). "Input-output parametric models for nonlinear systems -part I: deterministic nonlinear systems." Int J. of Control **41**: 303-328.
- Leontaritis, I. J. and S. A. Billings (1985). "Input-output parametric models for nonlinear systems -part II: stochastic nonlinear systems." Int J. of Control **41**: 329-344.
- Mayhew, J., L. Zhao, et al. (1997). "Spectroscopic investigation of the reflectance changes in barrel cortex following whisker stimulation." Advances in Experimental Medicine and Biology (in press).
- Mayhew, J. E. W., S. Askew, et al. (1996). "Cerebral vasomotion: 0.1Hz oscillation in reflected light imaging of neural activity." Neuroimage **4**: 183-193.
- Mindlin, G. B. and R. Gilmore (1992). "Topological analysis and synthesis of chaotic time series." Physica D **58**: 229-242.
- Rosenstein, M. T., C. J.J., et al. (1993). "A practical method for calculating largest Lyapunov exponents from small data sets." Physica D **65**: 117-134.
- Schmidt, J. A., P.Borgstrom, et al. (1993). Vasomotion as a flow dependent phenomenon. Vasomotion and Flow Motion. Prog Appl.Microcirc. C. Allegra, M. Intaglietta and K. Messmer. Basel, Karger. **20**: 34-51.
- Theiler, J., S. Eubank, et al. (1992). "Testing for nonlinearity in time series: the method of surrogate data." Physica D **58**: 77-94.
- Tsuda, I., T. Tahara, et al. (1992). "Chaotic pulsation in human capillary vessels and its dependence on mental and physical conditions." International Journal of Bifurcation and Chaos **2**: 313-324.
- Wiedeman, M. P. (1957). "Effect of Venous Flow on Frequency of Venous Vasomotion in the Bat Wing." Circulation Research **5**: 641-644.

List of figures

Figure 1: Raw (dotted) and smoothed (cont.) data recorded under (a) green and (b) red illumination

Figure 2: Correlation Dimension vs. $\log(r)$ for (a) experimental data and (b) for the surrogate signal.

Figure 3: Close Return Map of the (a) experimental signal and (b) surrogate data

Figure 4: Limit Cycle behaviour of the autonomous model.

Figure 5: Phase-space portrait plotted using (a) experimental data and (b) the model simulated outputs

Figure 6: One-step-ahead model predicted outputs (dash-dot) superimposed on the estimation data (a) under green illumination and (b) under red illumination

Figure 7: Model simulated outputs (dash-dot) superimposed on the estimation data (a) under green illumination and (b) under red illumination

Figure 8: Correlation Dimension vs. $\log(r)$ plot for the estimated model

Figure 9: Close Return Map computed using the model predicted output

Figure 10: Poincaré Map plot for the estimated model

Figure 11: (a) spectral variation in the V-signal over time, (b) time series of the absorption at 570nm and 650nm and (c) the absorption changes due to the oscillation in the tissue scattering obtained using Nonlinear Multi-Component Analysis (NLMCA). In (c) changes in cytochrome oxidation and in oxygenated haemoglobin are superimposed on the difference between the red and green V-signal measurements.

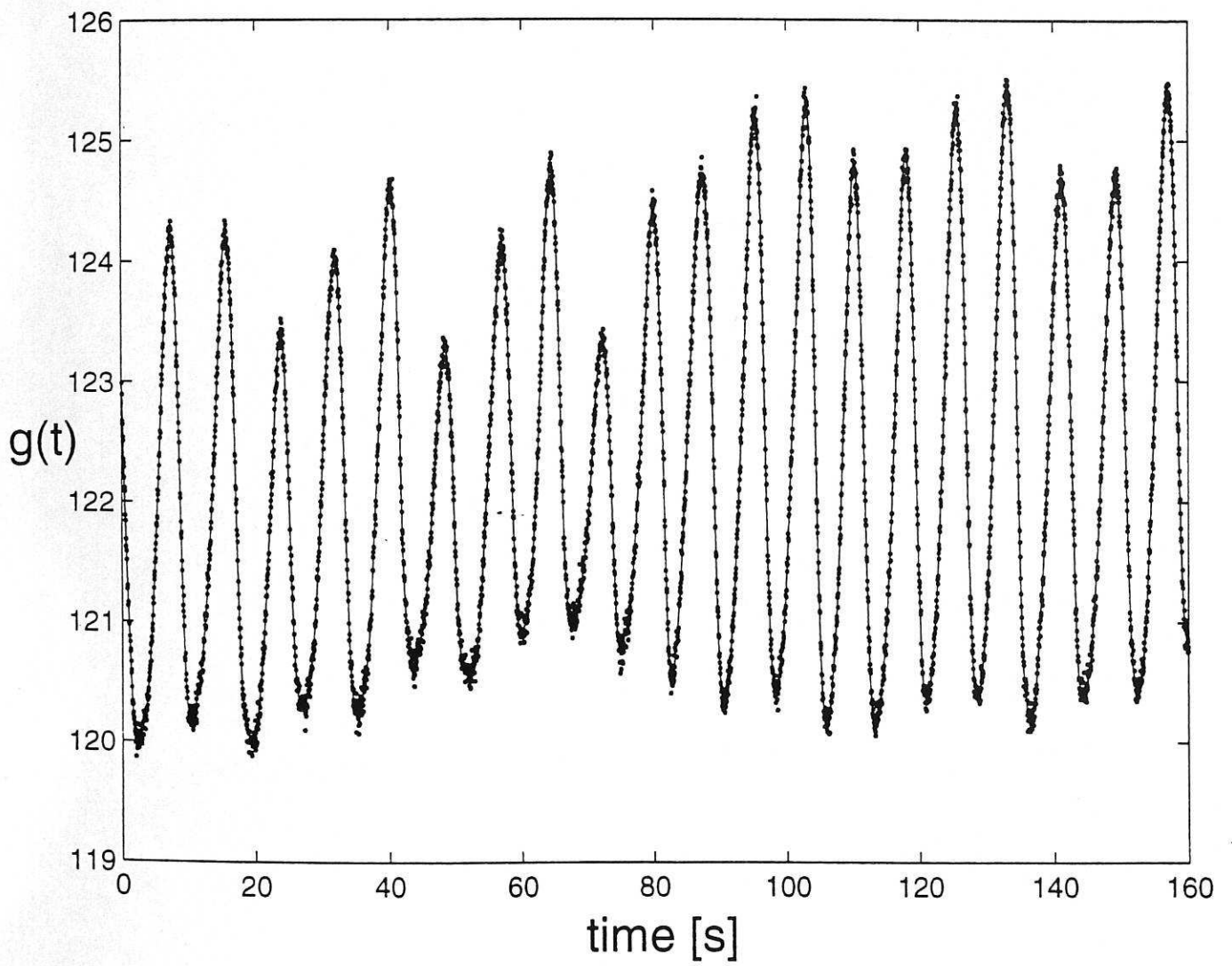


FIG. 10

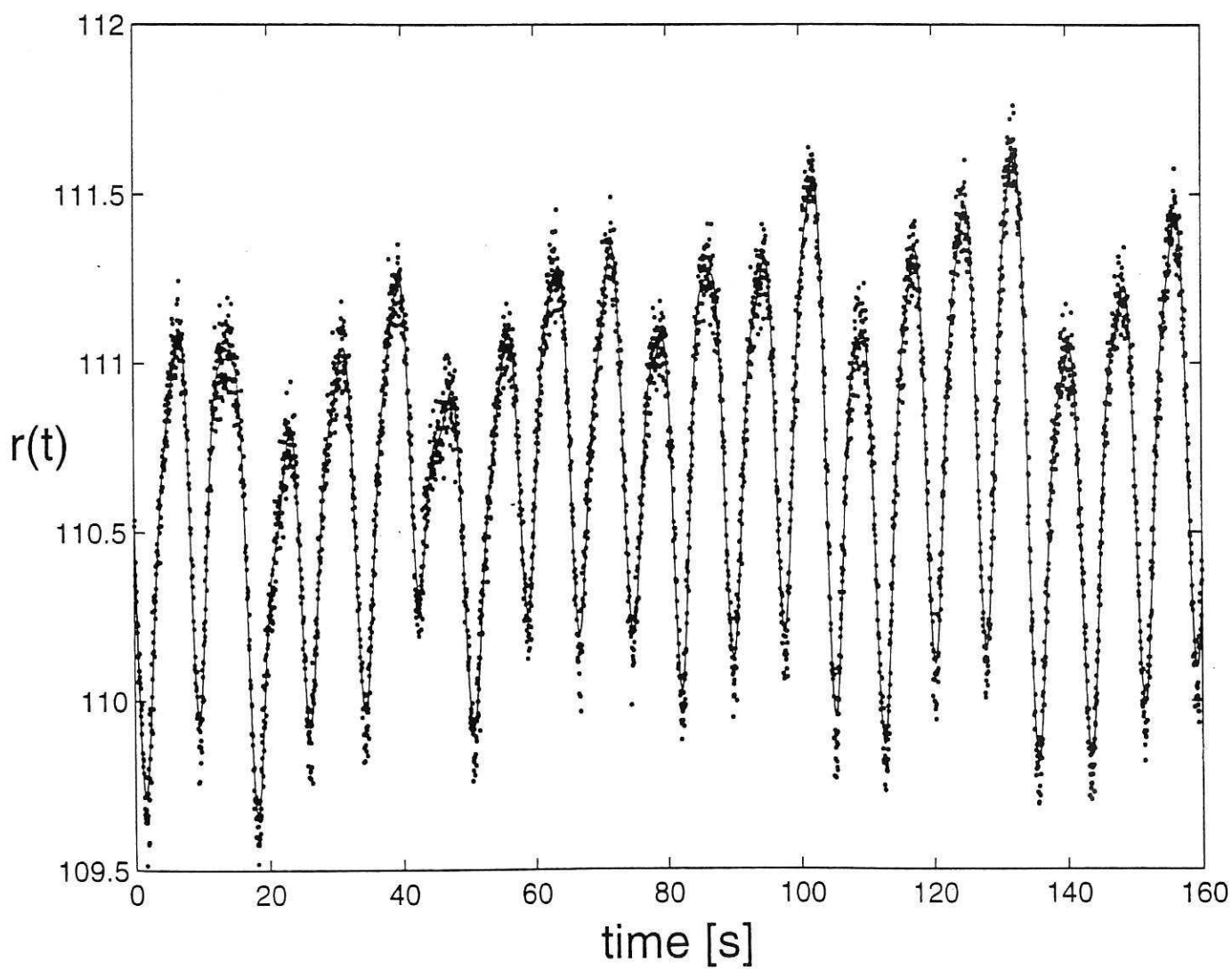


FIG. 10

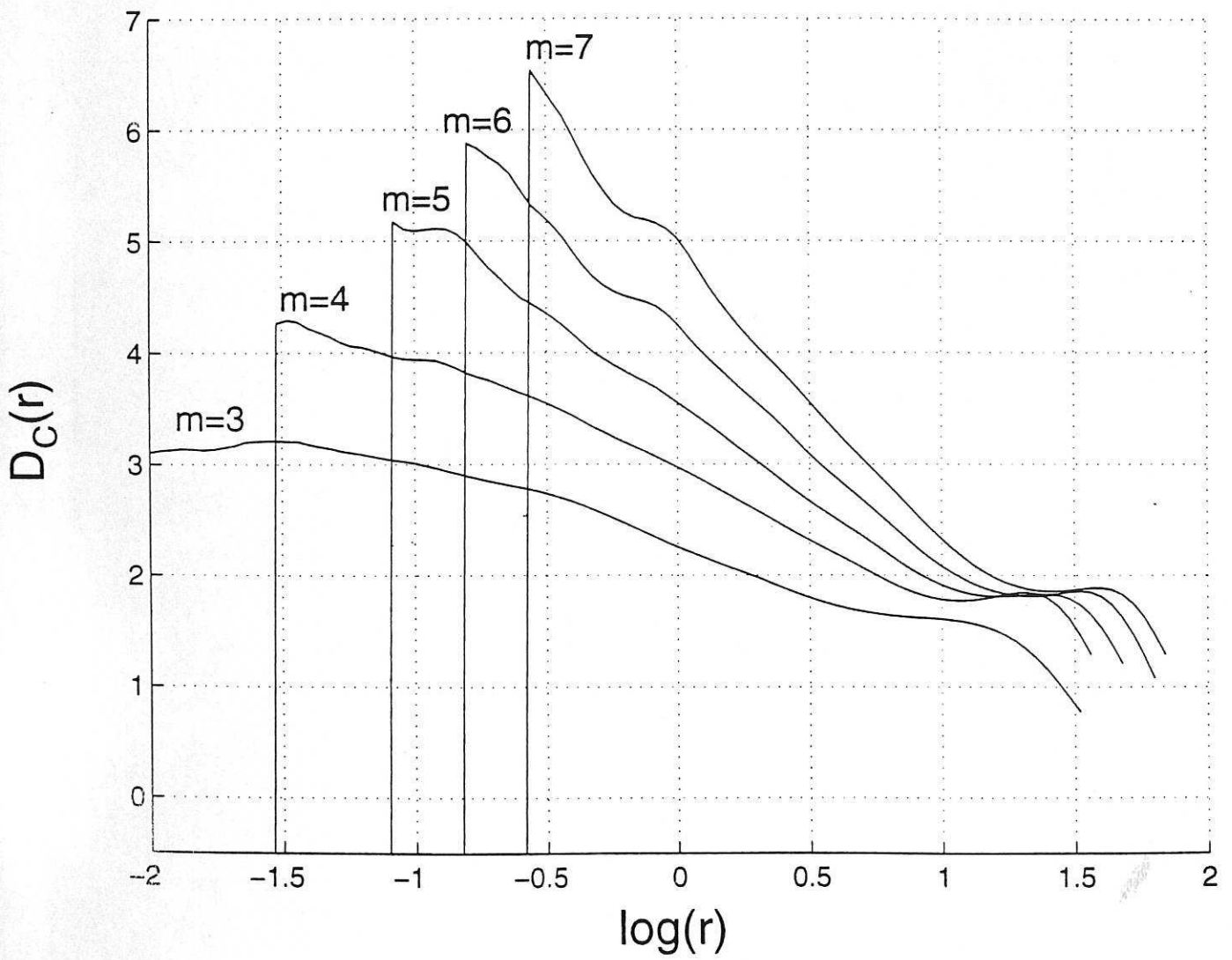


Fig. 2.3

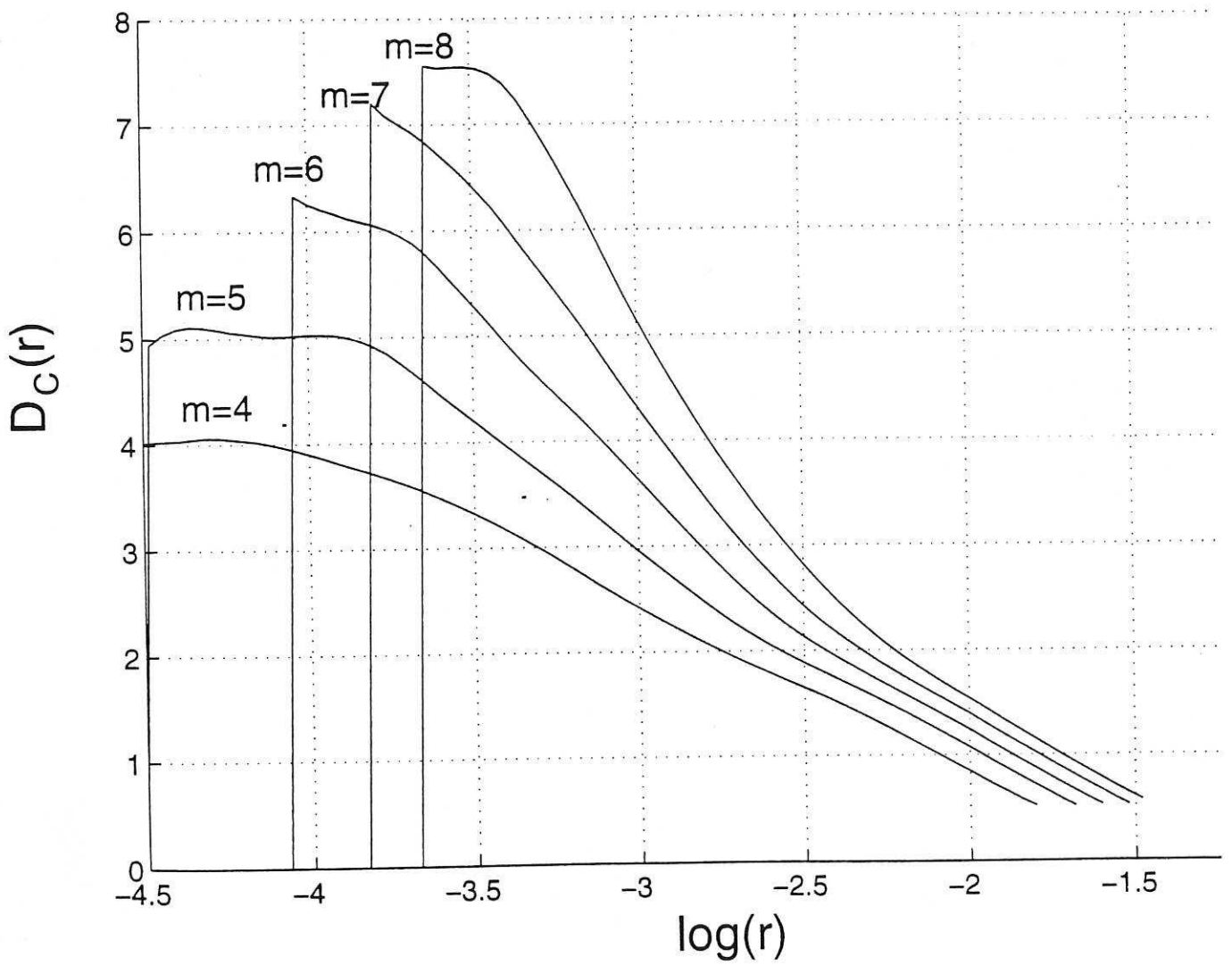


FIG. 26

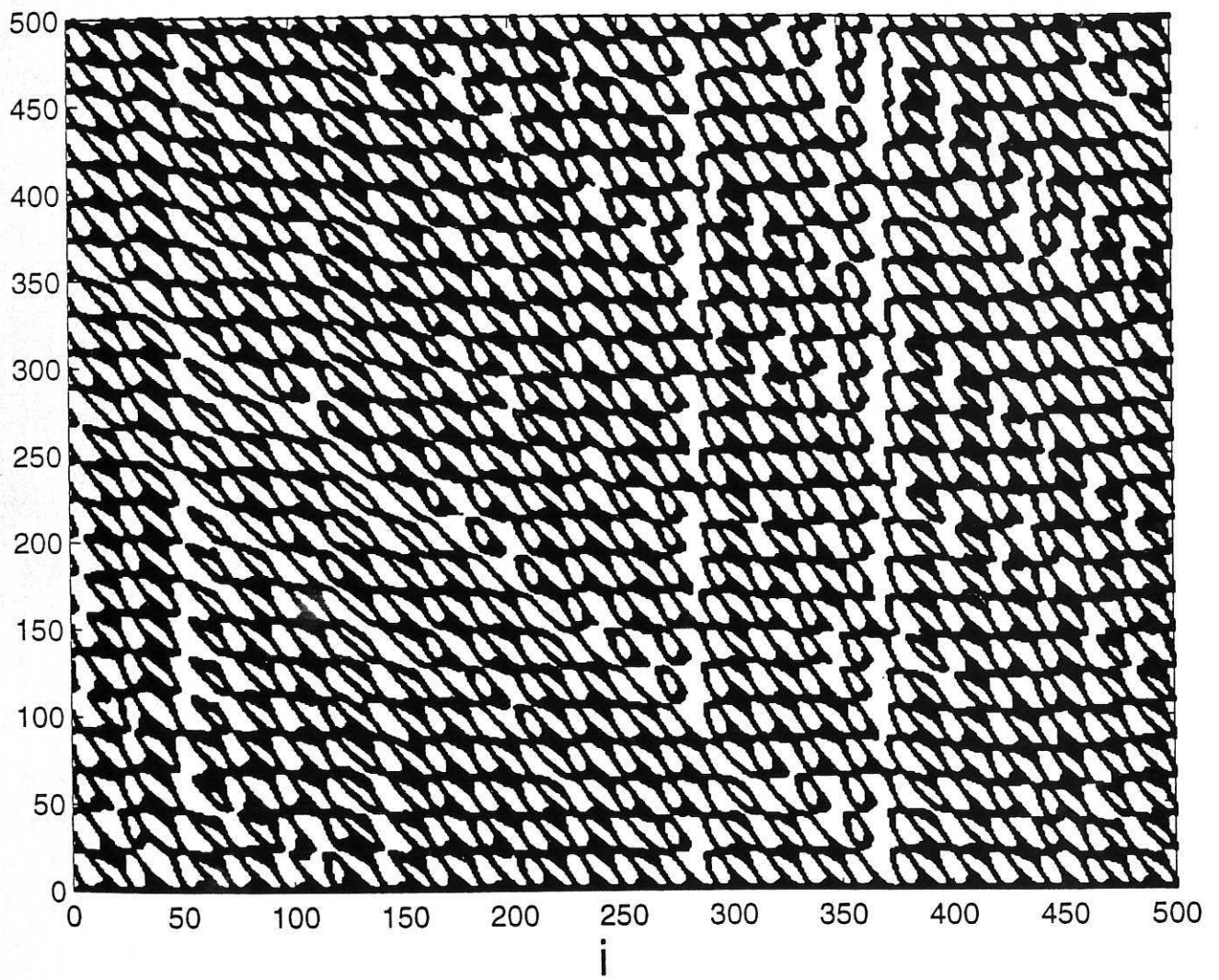


Fig. 30

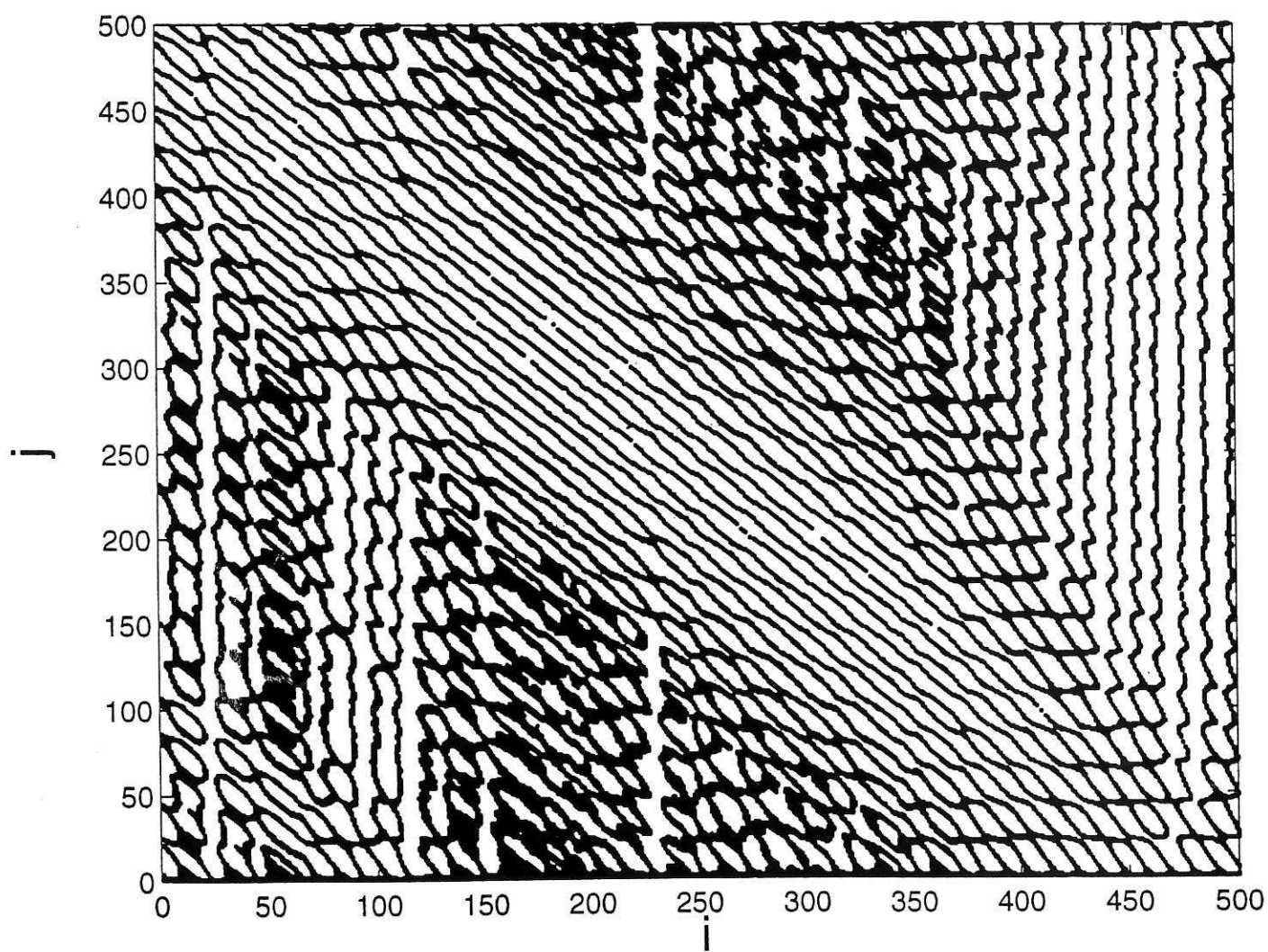


FIG. 30

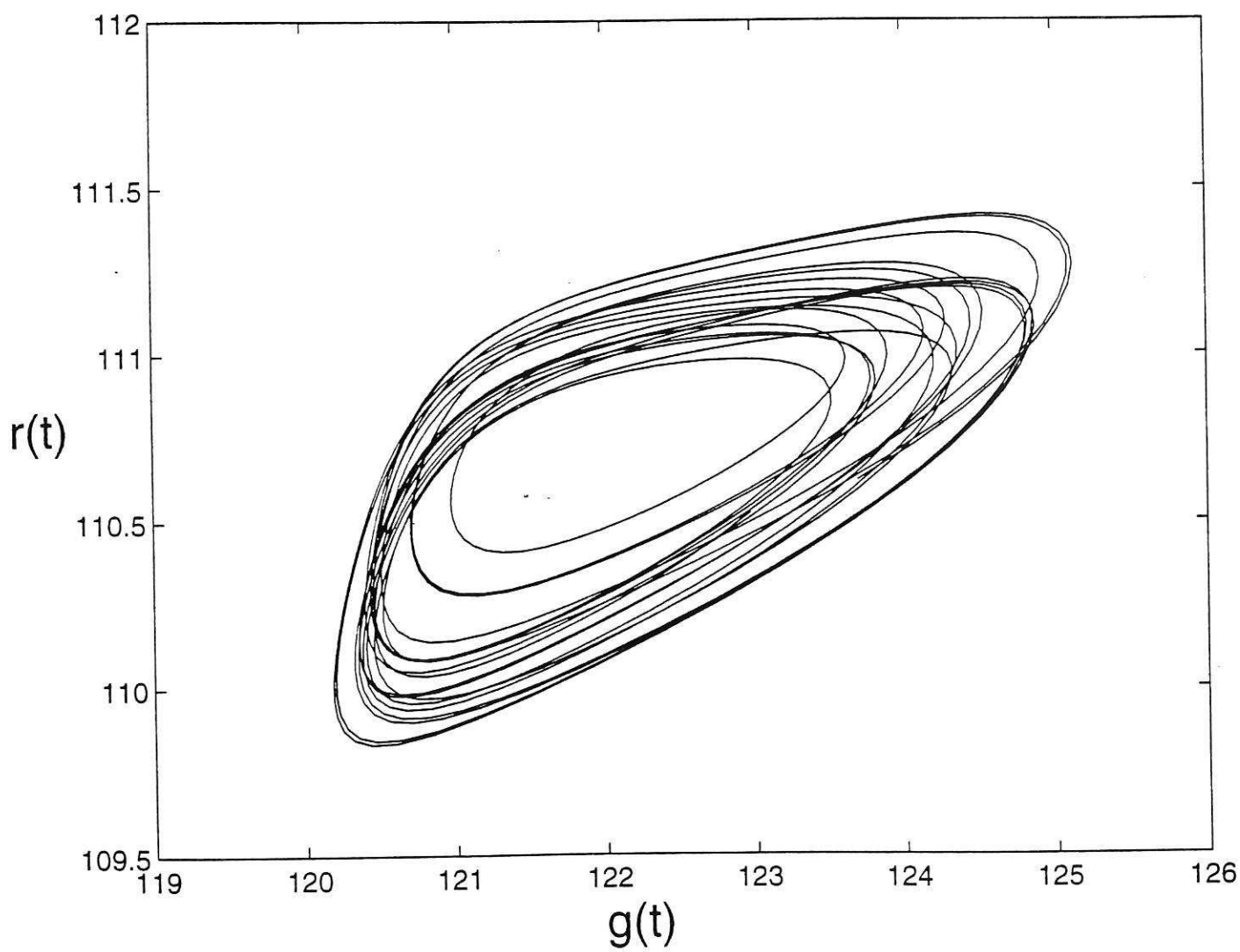
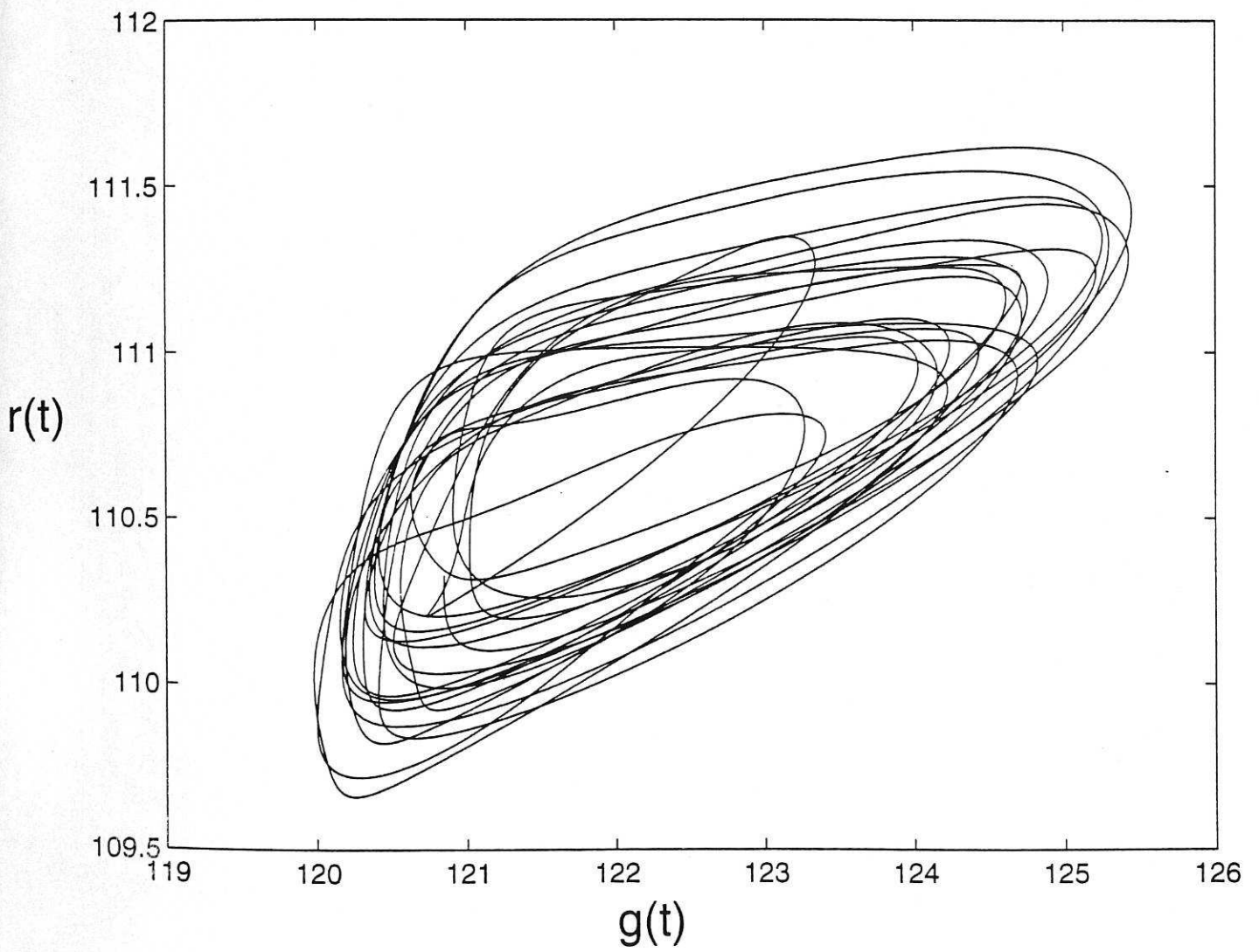
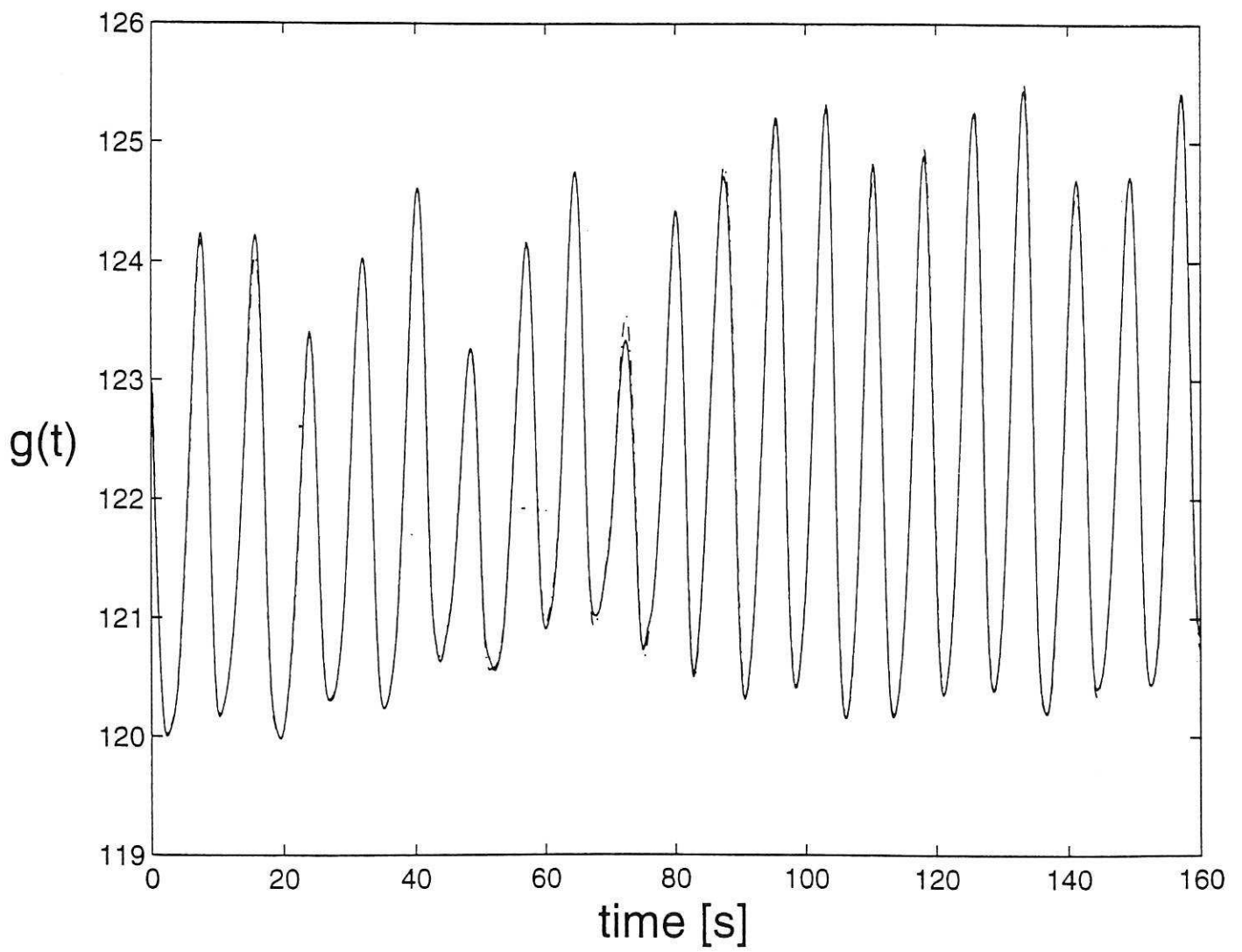


FIG. 5a



111.5



#75, 60

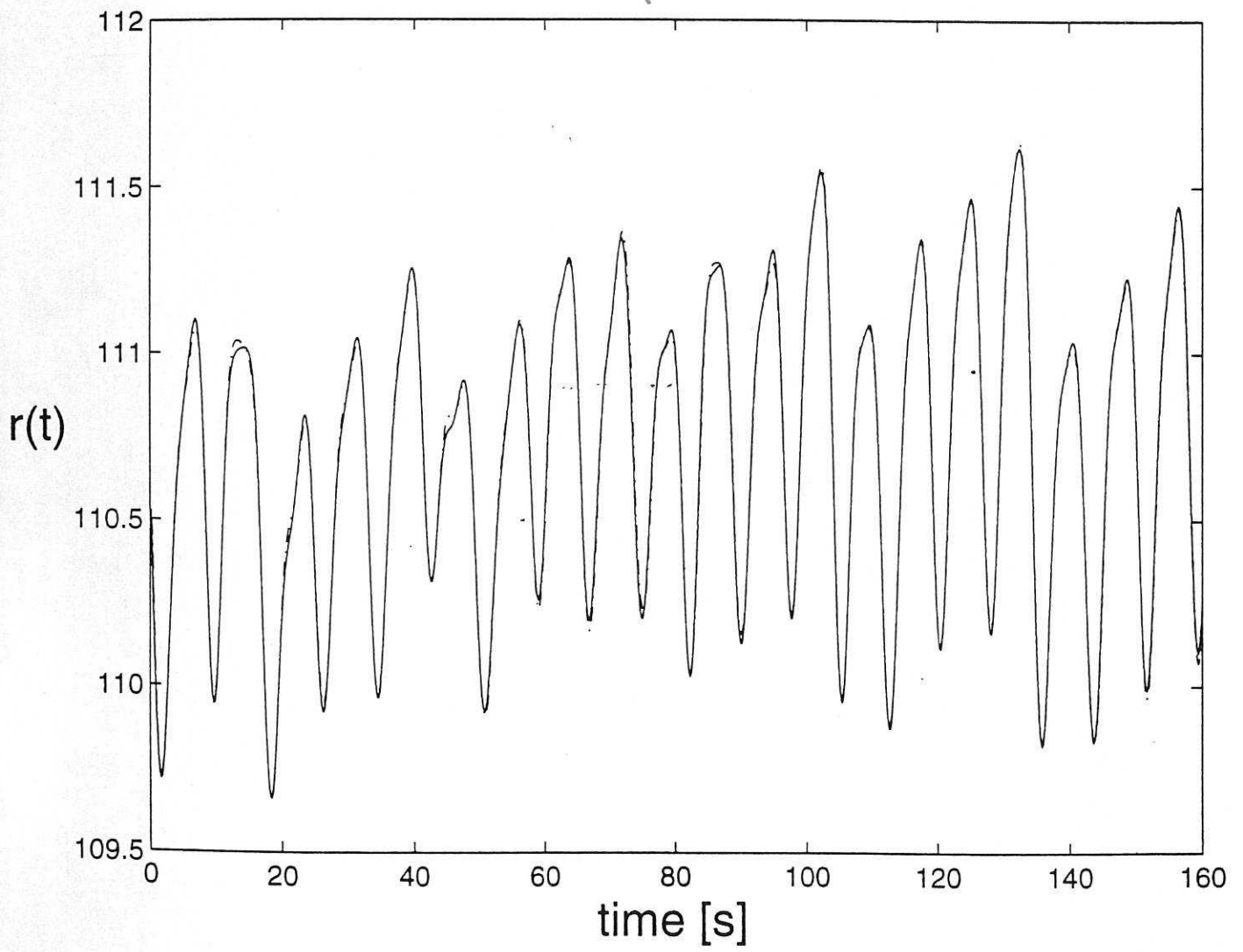


FIG. 5b

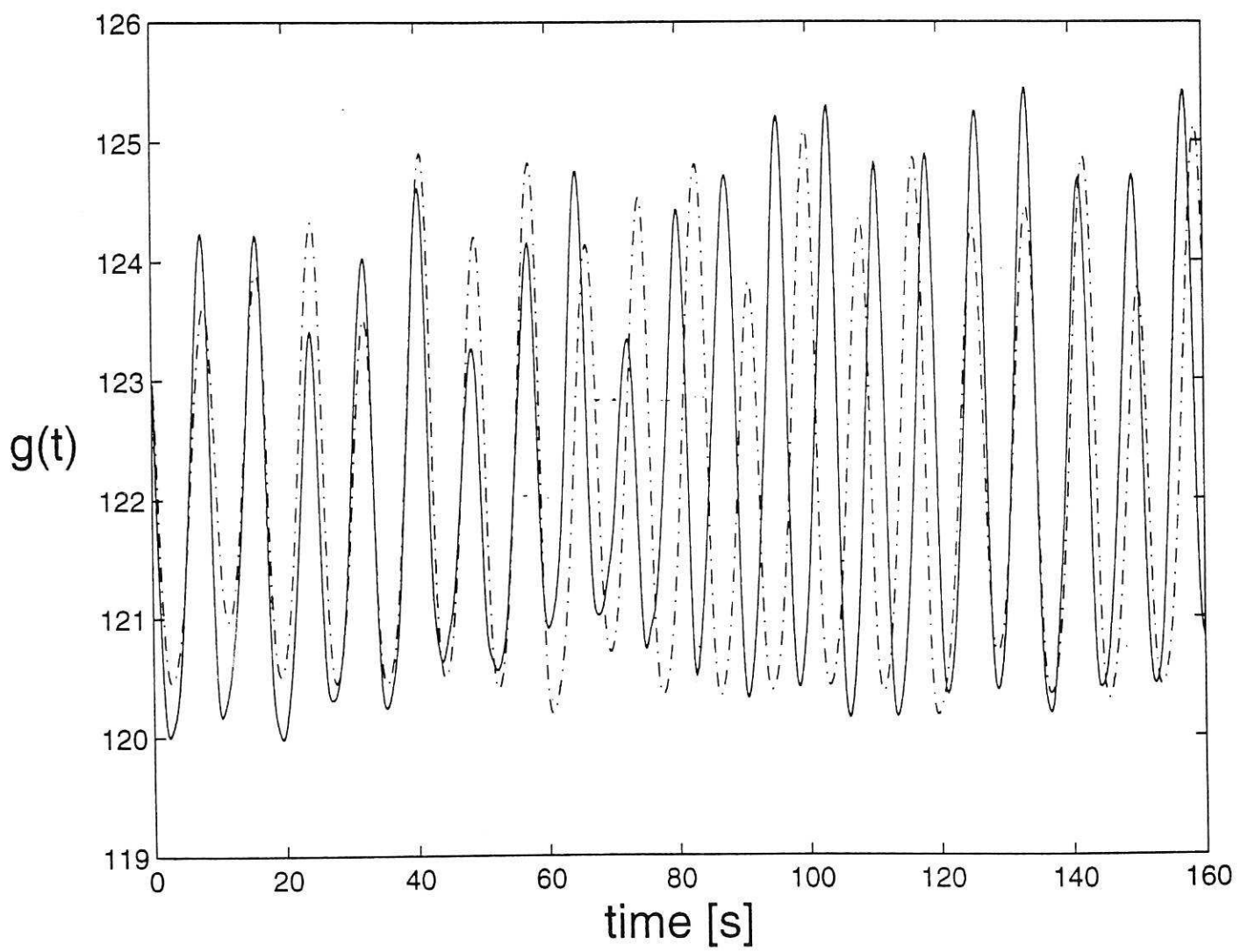


Fig. 70

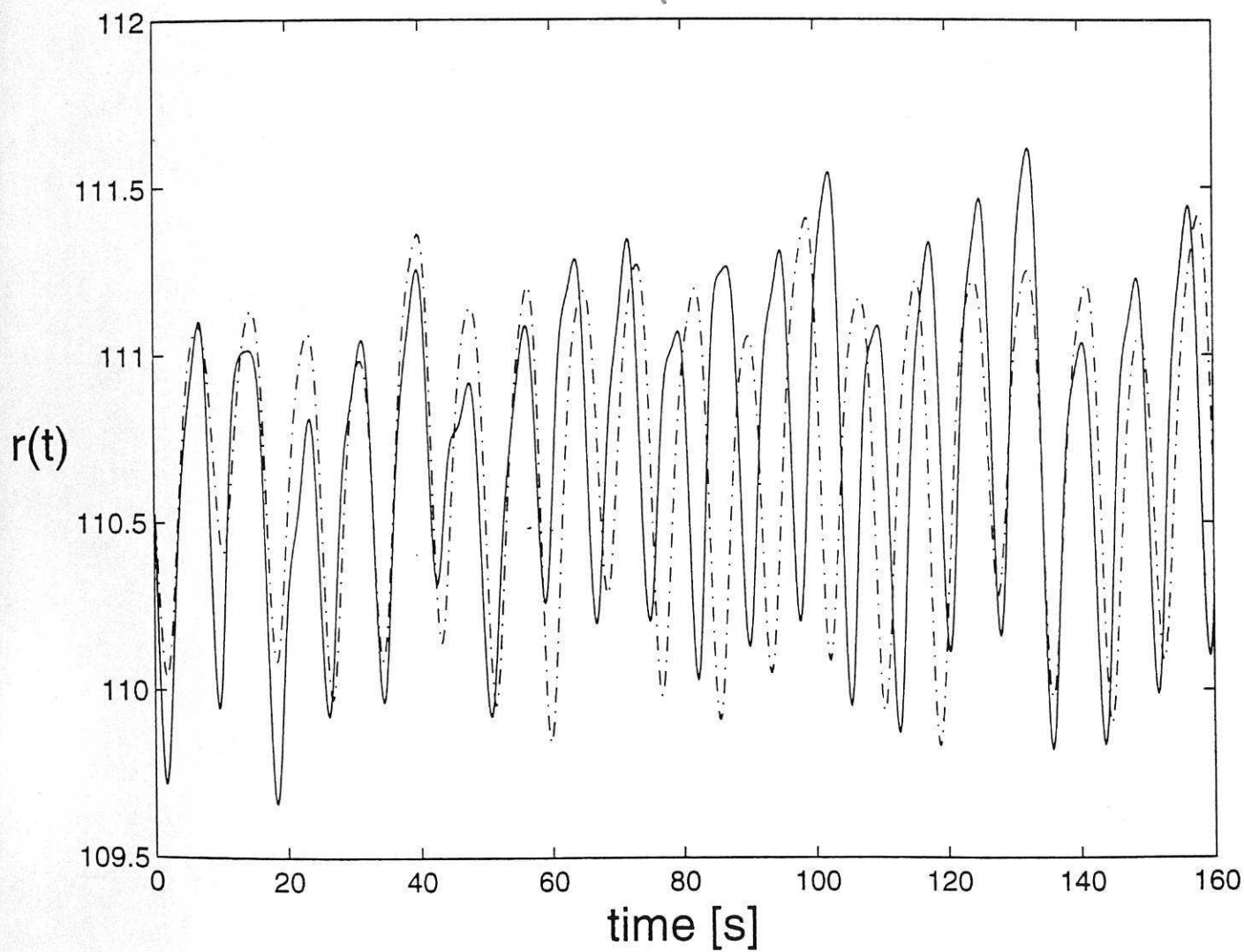


FIG. 30

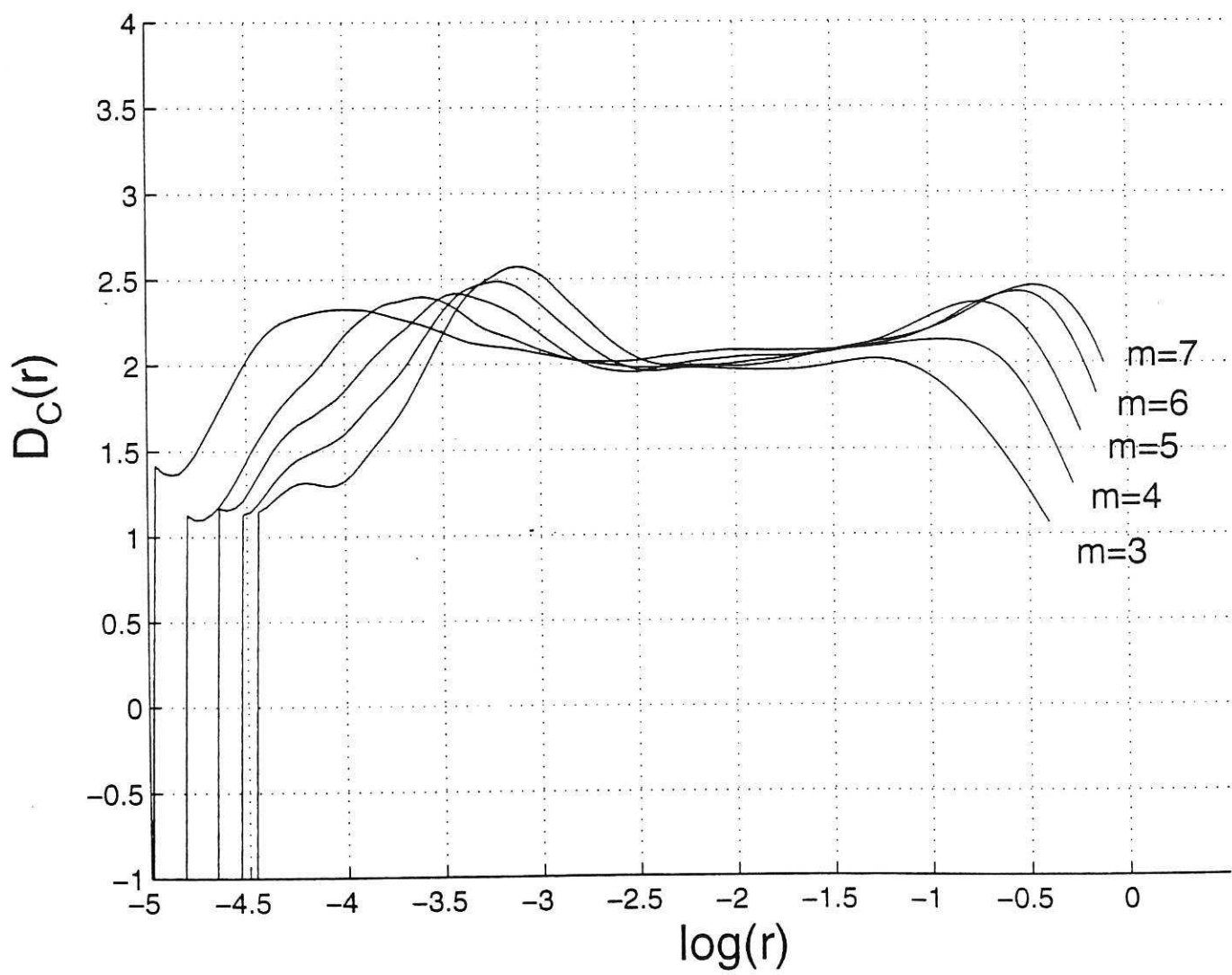


FIG. 8

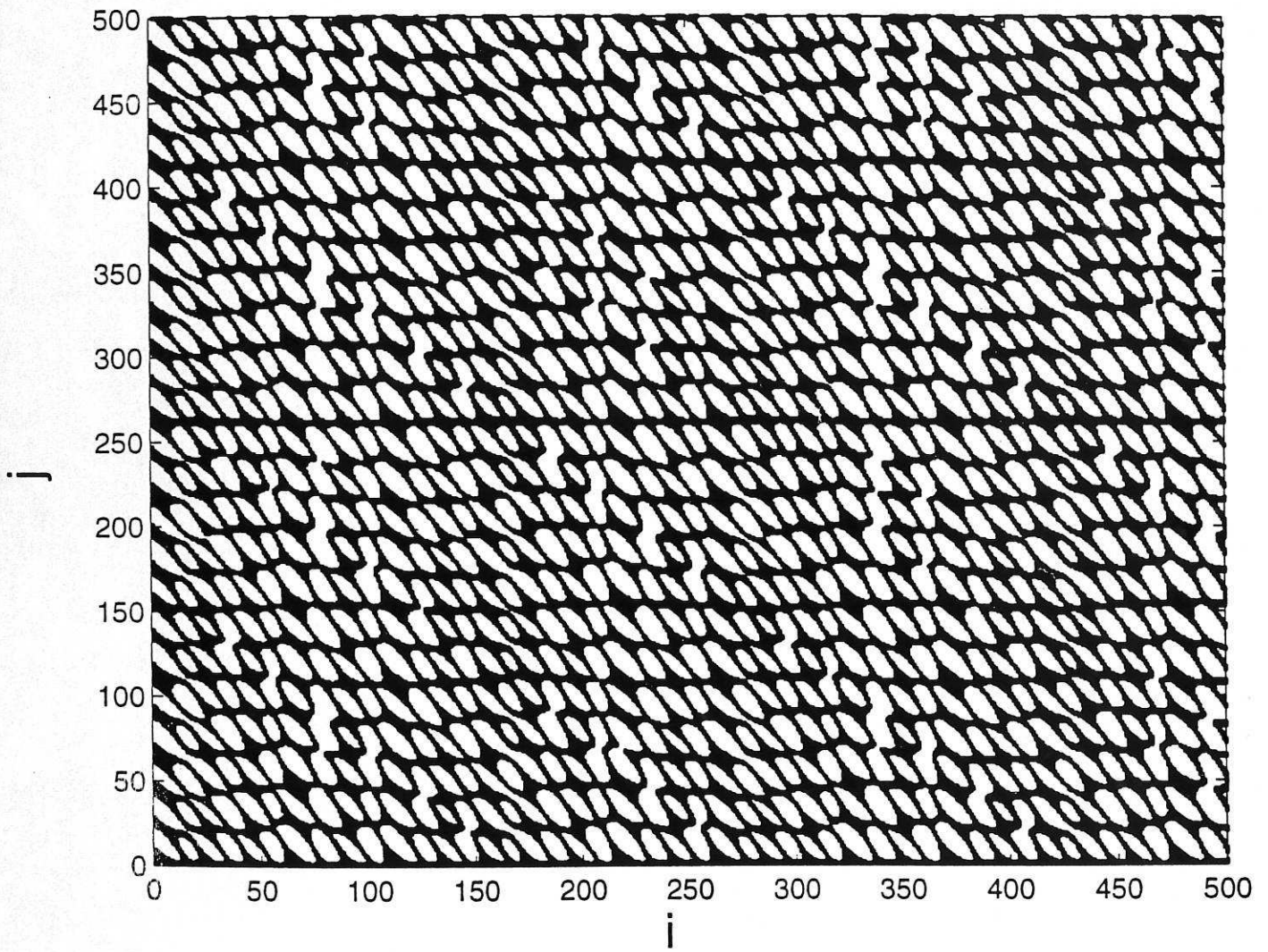


FIG. 9

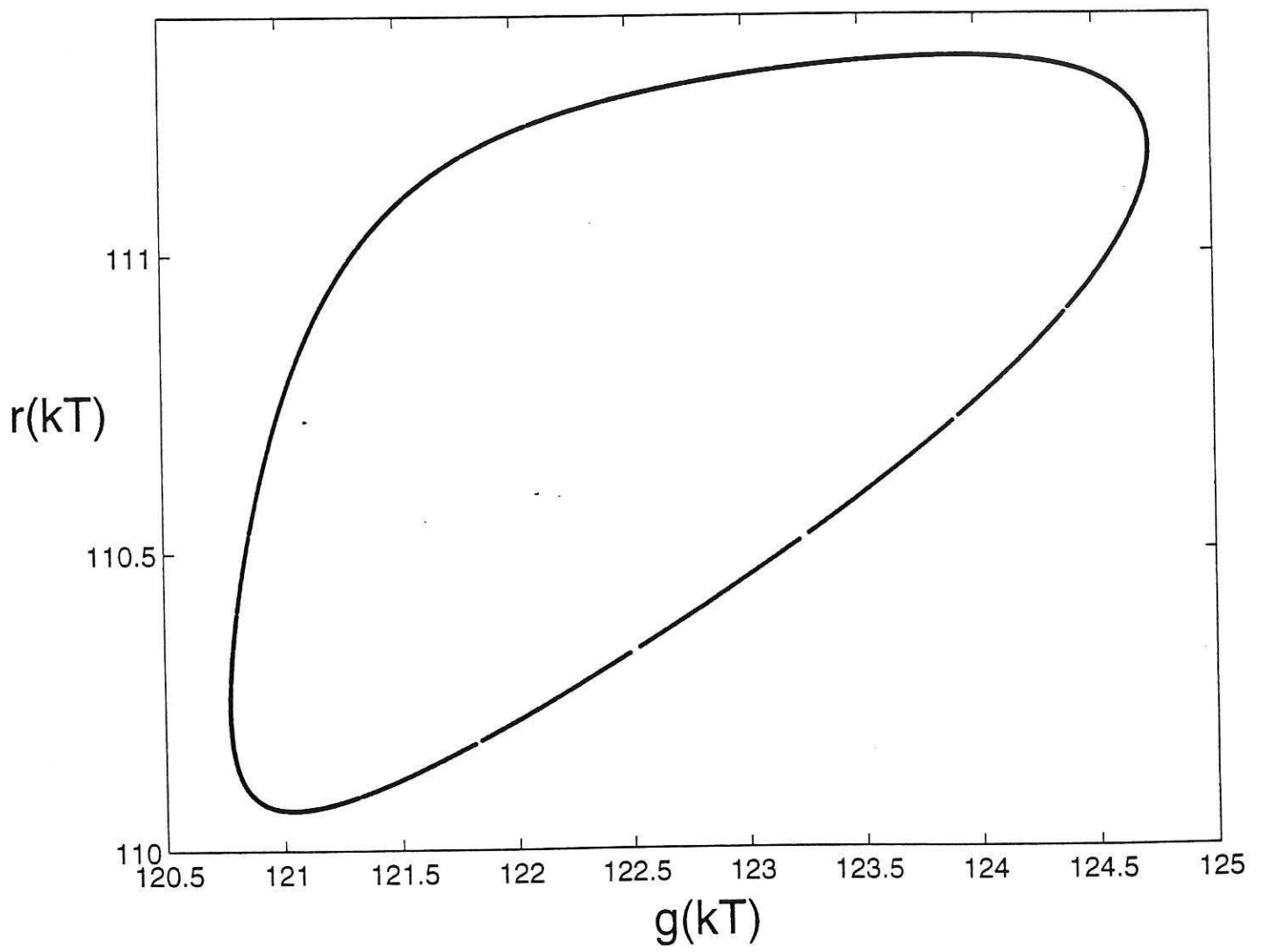


FIG. 10

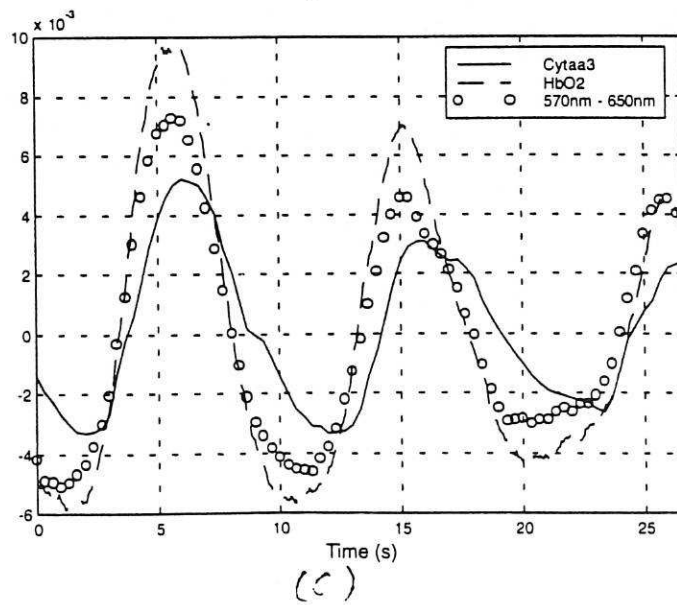
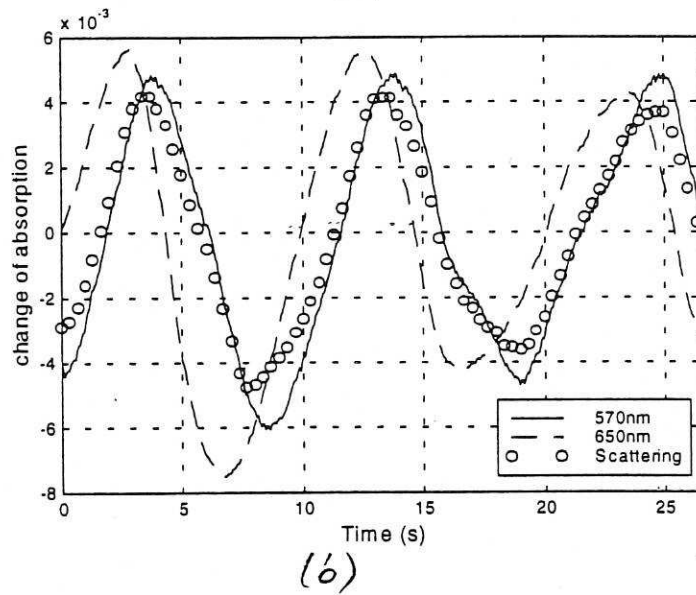
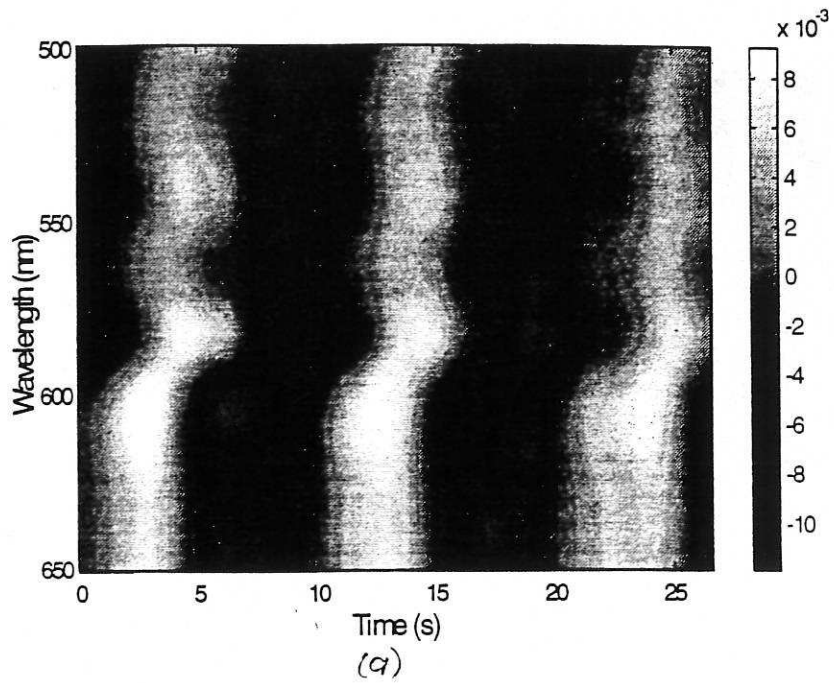


FIG. 11

